DALTON

What can calculations employing empirical potentials teach us about bare transition-metal clusters?†

David J. Wales,* Lindsey J. Munro and Jonathan P. K. Doye

University Chemical Laboratories, Lensfield Road, Cambridge CB2 1EW, UK

The implications for transition-metal clusters of theoretical results for systems containing 10–148 atoms bound by empirical potentials have been considered. The effects of the range of the interatomic pair potential and anisotropy on the potential-energy surface are now quite well understood. For example, as the range decreases the favoured morphology changes from icosahedral to decahedral and then to cuboctahedral. Since strain increases with size the crossover between electronic and geometrical 'magic numbers' exhibited by alkali-metal clusters can be rationalised. Calculations employing specific potentials designed to represent face-centred-cubic transition metals enable the study of changes in morphology and surface migrations in clusters of these elements. Single-step mechanisms exist for highly co-operative rearrangements between different structures, but the associated barriers scale as the total number of atoms. Hence, at larger size the same mechanisms are mediated by a series of transition states. The barriers for surface processes are comparable to those deduced experimentally and theoretically for bulk surfaces. It is predicted that icosahedral order is 'frozen in' at relatively small size and Mackay icosahedra grow *via* anti-Mackay and then Mackay overlayers.

In this contribution we consider some of the ways in which calculations based upon empirical potentials can provide new insight into the structure and dynamics of bare transition-metal clusters. Very large *ab initio* calculations on systems such as bare and ligated Au_{55} clusters[1] (including relativistic effects) and large fullerenes[2–4] (using Yang's 'divide-and-conquer' approach) have recently become feasible. However, to survey a multidimensional potential-energy surface (PES) in detail and characterise low-lying minima, transition states and reaction pathways for a cluster containing tens of transition-metal atoms would be extremely computationally expensive. Since the number of minima appears to scale exponentially with the number of atoms[5–7] even finding the global potential-energy minimum rapidly becomes a difficult task.

We therefore consider two simple potentials which each have only one free parameter corresponding to anisotropy and range, respectively, and two classes of empirical many-body potentials fitted to specific face-centred-cubic (f.c.c.) transition metals. Our results are most relevant to molecular-beam studies such as the recent flow-tube reactor experiments of Parks and co-workers.[8–13] In this work the number of active binding sites of different kinds, and hence the structure of the cluster, is deduced from the characteristics of ligand uptake. Comparisons of our results with previous calculations[14,15] and, where appropriate, with results for surface processes are also possible. The original aspects of this paper are primarily our comparisons of the trends found for the different potentials and our analysis of nickel clusters in the light of recent flow-tube results (third section). Details of the geometry optimisations and reaction-path calculations are omitted but may be found elsewhere.[16]

A Model Anisotropic Potential

The Lennard–Jones[17] (LJ) potential has the form (1) where r_{ij}

$$V = 4\varepsilon \sum_{i<j} \left[\left(\frac{\sigma}{r_{ij}} \right)^{12} - \left(\frac{\sigma}{r_{ij}} \right)^{6} \right] \qquad (1)$$

is the separation of atoms i and j, ε the pair-potential well depth and σ the separation where the pair interaction goes through zero. However, once ε and σ are chosen as the units of energy and distance there are no adjustable parameters. Furthermore, pairwise additive potentials are well known to be inadequate in providing a description of transition metals which do not generally obey the Cauchy relation, for example.[18] A simple anisotropic form is obtained[19] by adding the Axilrod–Teller[20] (AT) triple-dipole three-body term, equation (2), where θ_1, θ_2

$$V = 4\varepsilon \sum_{i<j} \left[\left(\frac{\sigma}{r_{ij}} \right)^{12} - \left(\frac{\sigma}{r_{ij}} \right)^{6} \right] + Z \sum_{i<j<k} \left[\frac{1 + 3\cos\theta_1 \cos\theta_2 \cos\theta_3}{(r_{ij} r_{ik} r_{jk})^3} \right] \qquad (2)$$

and θ_3 are the internal angles of the triangle Δijk and Z is the parameter which specifies the magnitude of the three-body term. If we use a reduced unit system in which ε is the unit of energy and σ the unit of length then there is just one adjustable parameter left, namely $Z^* = Z\sigma^9/\varepsilon$. Previous applications of this potential have been made to both main-group and metal clusters and solids.[19]

We have previously considered the effect of Z^* on the topography of the PES systematically for small clusters[21] and for some larger metal clusters.[22] Negative values of Z^* reinforce the LJ term and do not result in a qualitative change of the PES. However, for positive Z^* the three-body term destabilises triangles and favours linear arrangements of atoms. For sufficiently large values of Z^* the LJAT potential supports rings and chains.[21] A systematic survey for six-atom clusters[21] showed that dozens of new stationary points occur as Z^* varies from zero to 3.0. Fig. 1 shows all the non-planar minima and the transition states which link them to other minima that were found in this study. The use we envisage for this result is to provide a first guess at how newly characterised clusters might rearrange. This entails finding a range of Z^* over which the known geometry is stable for the LJAT potential and then considering the rearrangements that the model cluster undergoes. In effect this procedure fits the value of Z^* so that the experimental geometry is known to be supported as a minimum (this is a more stringent condition than is generally appreciated). Most of the observed mechanisms can be

† Basis of the presentation given at Dalton Discussion No. 1, 3rd–5th January 1996, University of Southampton, UK.

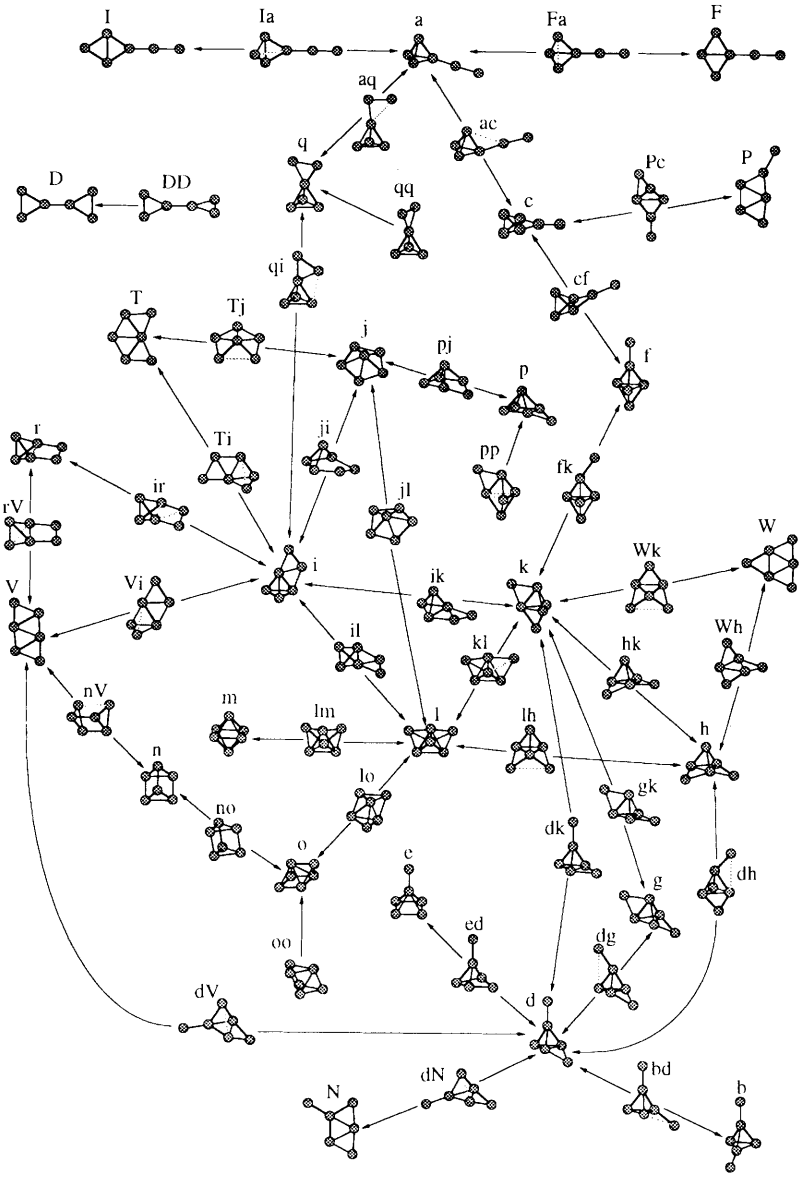

Fig. 1 Interconnections between all the non-planar minima and transition states found for a six-atom cluster bound by the LJAT potential. These structures do not all generally exist for a given value of Z^*

classified as diamond–square–diamond (DSD) type[23] [Fig. 2(*a*)] or edge-bridging[24] [Fig. 2(*b*)], although some others were also found [see, for example, Fig. 2(*c*)].[21]

The structural properties of 13-, 55-, 147- and 309-atom Mackay icosahedra,[25] Ino decahedra[26] and cuboctahedra have also been analysed for the LJAT potential.[22] At each of these sizes, known as 'magic numbers', high-symmetry structures belonging to point groups I_h, D_{5h} and O_h are completed, as shown in Fig. 3. The Ino decahedron is obtained by truncating a pentagonal bipyramid to give five new {100}-type square faces. Of course, this means that the structure now has more than ten facets, but it is usual to call such clusters 'decahedral' in view of the aforementioned construction. For each size the icosahedron lies lowest in energy, followed by the decahedron. However, these structures contain five-fold rotation axes, and therefore cannot pack indefinitely without incurring excessive strain, hence crossovers in stability must occur with increasing size. Our general result is that as Z^* increases these crossovers occur at smaller size.[22] This is easily rationalised by considering the number of {111}- and {100}-type surface facets in each structure. If we attempt to fit bulk properties using the single free parameter our results are generally in the range $0.1 < Z^* < 0.35$, although accurate fits are certainly not possible. Transmission electron microscope results for small metal particles on supports, summarised in ref. 22, suggest that

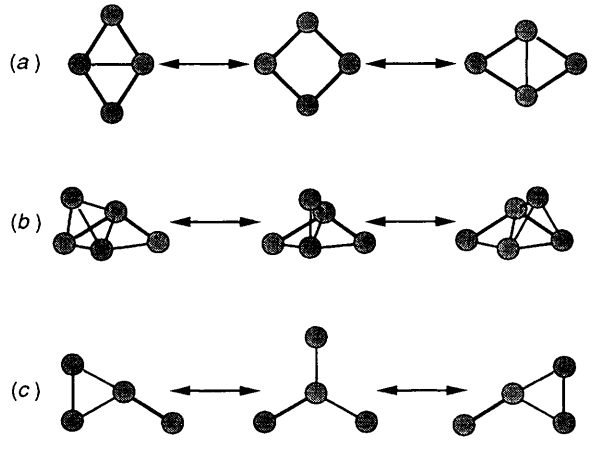

Fig. 2 Mechanisms found for six-atom LJAT clusters: (*a*) diamond–square–diamond process, (*b*) edge-bridging process and (*c*) edge-bridged-terminal–edge-bridged process

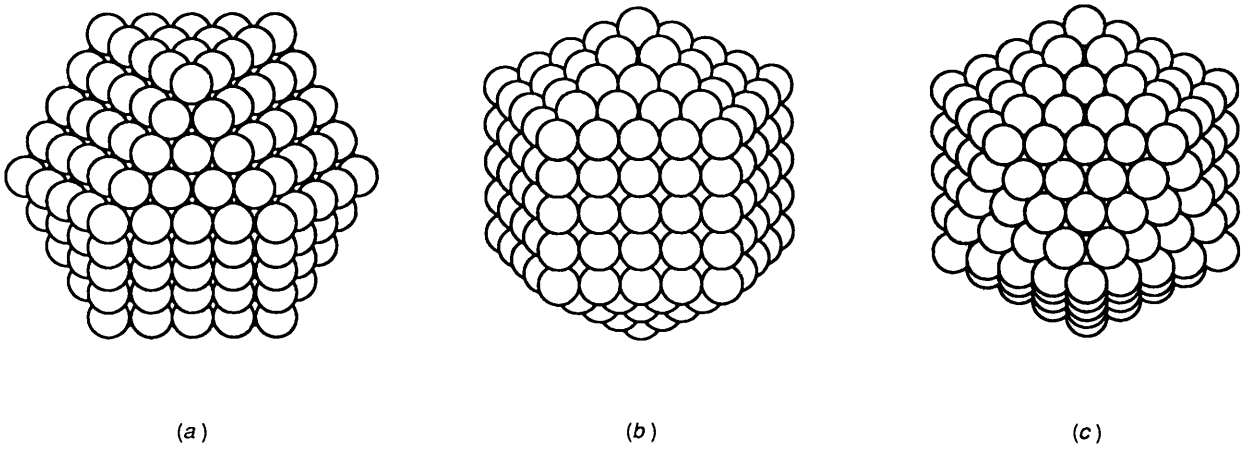

Fig. 3 561-Atom clusters: (*a*) f.c.c. cuboctahedron, (*b*) Ino decahedron and (*c*) Mackay icosahedron

Table 1 The Morse range parameter ρ_0 for various fits

Metal	Bulk fit[a]	Diatomic fit[b]	Sutton–Chen[c] (SC)	Murrell–Mottram[c] (MM)
Na	3.15	—	—	—
K	3.17	—	—	—
Rb	3.10	—	—	—
Cs	3.14	—	—	—
Mg		4.16	—	—
Ca	3.68	4.70	—	—
Sr	3.68	—	—	—
Ba	3.53	—	—	—
Cr	4.33	—	—	—
Mo	4.49	—	—	—
W	4.28	—	—	—
Fe	3.95	—	—	—
Rh	—	—	6.00	—
Ni	3.95	—	5.20	—
Pt		—	6.33	—
Cu	3.89	3.13	5.20	5.50
Ag	4.27	3.68	6.00	6.00
Au	—	4.18	6.33	7.00
Al	3.79	—	—	—
Pb	4.42	—	—	—
Ne	—	2.05	—	—
Ar	—	5.72	—	—
Kr	—	6.81	—	—
Xe	—	6.67	—	—

[a] Obtained by fitting to the experimental vaporisation energy, lattice constant and compressibility.[28] [b] Obtained by fitting to spectroscopic data for diatomic molecules.[29] [c] From analytical calculations.

smaller values of Z^* are appropriate for Au and Ag, intermediate values for Pd and Cu, and relatively large values for Pt, where the cuboctahedral morphology appears to dominate for particles of diameter 10–100 Å. We also find surface contractions of a reasonable magnitude (compared to results for bulk surfaces) for the same range of Z^* values.[22]

The Morse Potential

We now consider clusters bound by the Morse potential[27] which may be written as in equation (3) where $\varepsilon = 1$ and $r_0 = 1$

$$V_M = \varepsilon \sum_{i<j} e^{\beta(r_0 - r_{ij})}[e^{\beta(r_0 - r_{ij})} - 2] \equiv \sum_{i<j} e^{\rho_0(1 - r'_{ij})}[e^{\rho_0(1 - r'_{ij})} - 2] \quad (3)$$

define the units of energy and length respectively, $\rho_0 = \beta r_0$ and r'_{ij} denotes the distance between atoms i and j in these reduced

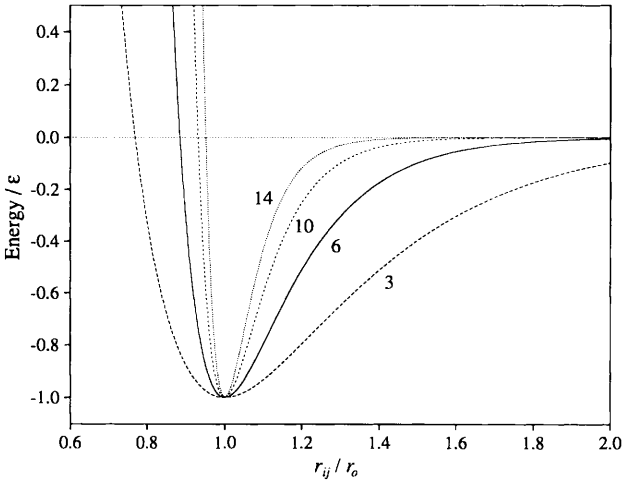

Fig. 4 Plots of the Morse potential for a range of ρ_0 values

units. Morse clusters will be denoted M_N. Compared to the simple LJ potential we again have one free parameter, ρ_0, which determines the range of the attractive part of the potential. As shown in Fig. 4, decreasing ρ_0 increases the range of the attractive part of the potential and softens the repulsive wall, widening the potential well. For comparison, $\rho_0 = 6$ matches the curvature of the LJ potential at the bottom of the well, and at this value the Morse and LJ PES's are very similar. Some other best-fit values are given in Table 1 from various sources; note that the relative values in each column are in reasonable agreement.

In previous work Braier *et al.*[30] made a systematic search of the PES for M_6 and M_7 as a function of the range. They found that the PES became more complex, *i.e.* supported more minima and transition states, as the range of the potential decreased. This is easily understood since the short range of the potential means that distant atoms are far less sensitive to one-another's precise positions, and has been noted by other workers.[5,31,32] The simplification of the PES at long range led Stillinger and Stillinger[33] to suggest that this approach might be used for global minimisation by hypersurface deformation,[34] but this now seems unlikely in the light of more systematic surveys of how the PES changes with ρ_0. Previous studies have also considered the effect of the range of the potential. Stave and DePristo[14] analysed their results for nickel and palladium clusters in terms of the range and Bytheway and Kepert[35] showed that icosahedral packing becomes less favourable than structures with higher co-ordination numbers for sufficiently long-ranged potentials.

Girifalco's model intermolecular potential for C_{60} is isotropic and exceptionally short-ranged relative to the

equilibrium pair separation;[36] the Morse potential which matches the curvature at the bottom of the well[37] has $\rho_0 = 13.62$. Not surprisingly, $(C_{60})_n$ clusters exhibit rather different properties from those of LJ clusters[16,38,39] and the bulk liquid phase is predicted to have only marginal stability[40] or none at all.[41] Here we consider M_N clusters with $7 \leqslant N \leqslant 25$ and a few additional sizes in the range $35 \leqslant N \leqslant 80$. We search for the global minimum as a function of N and ρ_0, and draw comparisons with previous work on bare metal clusters. Of course, since this is still a pair potential, we cannot expect to achieve quantitative agreement for any particular metal.

We partition the Morse potential into three contributions, equation (4), where the number of nearest-neighbour contacts

$$V_M = -n_{nn} + E_{strain} + E_{nnn} \quad (4)$$

is given by equation (5) with $x_{ij} = r'_{ij} - 1$ and x_0 is a nearest-

$$n_{nn} = \sum_{i<j, x_{ij}<x_0} 1 \quad (5)$$

neighbour cut-off. The strain energy, E_{strain}, is given by equation (6) and the contribution to the energy from non-

$$E_{strain} = \sum_{i<j, x_{ij}<x_0} (e^{-\rho_0 x_{ij}} - 1)^2 \quad (6)$$

nearest-neighbours, E_{nnn}, by equation (7). The most important

$$E_{nnn} = \sum_{i<j, x_{ij}>x_0} e^{-\rho_0 x_{ij}} (e^{-\rho_0 x_{ij}} - 2) \quad (7)$$

terms are n_{nn} and E_{strain}, and the formation of stable structures involves competition between the two since larger strains generally admit higher co-ordination numbers.[42] For given non-zero values of x_{ij}, which may be identified as the strains, E_{strain} increases rapidly with ρ_0, *i.e.* as the range decreases, because the potential well becomes narrower (Fig. 4). The effect of the range upon the relative stabilities of the icosahedron, decahedron and cuboctahedron is easily explained. In each case the interior atoms are twelve-co-ordinate, and so differences in n_{nn} arise from differences in the co-ordination of surface atoms. The icosahedron has only {111}-type faces and the cuboctahedron has the most {100} type, and therefore the smallest n_{nn}. At intermediate range the icosahedron therefore lies lowest of the three, and as ρ_0 increases first the decahedron and then the cuboctahedron become more favourable.

The smallest cluster for which we have found the global minimum to change as a function of range[42] is M_8. We have collected together all the structures that we believe to be global minima for some range of ρ_0 in Figs. 5–8 (except for the very smallest, which are well known). A detailed discussion of these structures is provided elsewhere;[42] here we will concentrate on comparing them with previous results.

Some of the structures we find at low ρ_0 are very similar to those reported by Stave and DePristo[14] in their studies of nickel and palladium clusters. In particular, their lowest-energy minima between 7 and 16 atoms correspond to our 7A–9A, 10B, 11C, 12B, 13A–16A (Figs. 5 and 6). The ranges of ρ_0 for which these structures are global minima[42] are generally in reasonable agreement with the value of $\rho_0 \approx 3.95$ for Ni in Table 1, suggesting that geometrical considerations, as opposed to electronic, play a significant role in determining the most stable structures even in this size range. Structures 8A–10A (Fig. 5) have relatively small values of n_{nn} but have favourable contributions from E_{nnn} because the next-nearest-neighbour shell is significantly closer than for structures based on icosahedra. These structures are roughly spherical and have the same shape as the boron skeletons of $B_8H_8^{2-}$, $B_9H_9^{2-}$ and $B_{10}H_{10}^{2-}$. Most of these minima are not based upon any identifiable regular structure, making prediction of low-energy structures at low ρ_0 rather hard.

For $N > 13$ growth can occur by capping the 13-atom icosahedron in two distinct ways, as shown in Fig. 9. The anti-Mackay overlayer[44] leads to the 45-atom rhombic tricontahedron[45] with I_h point-group symmetry,[46] and the Mackay overlayer leads to the 55-atom Mackay icosahedron.[25] The Mackay sites continue the f.c.c. close packing in each of the 20 distorted tetrahedra from which the icosahedron is constructed. Other authors have referred to the anti-Mackay overlayer as polyicosahedral,[47] because the growth sequence includes structures with interpenetrating icosahedra such as the double (19A) and triple (23A) icosahedra (Fig. 6). It has also been called the face-capping overlayer.[44] In LJ clusters the anti-Mackay overlayer is initially adopted in the series of global minima, and then for $N \geqslant 31$ the Mackay overlayer lies lower in energy.[44] The anti-Mackay overlayer results in more nearest neighbours but greater E_{strain} and hence the crossover to the Mackay overlayer occurs at smaller size as the range of the potential is decreased. For example, M_{24} and M_{25} are more stable with a Mackay overlayer for $\rho_0 = 10$. In contrast, alkali metals are expected to correspond to relatively long-ranged potentials (Table 1), and this is borne out in *ab initio* calculations for lithium clusters[48] where the anti-Mackay overlayer is lowest in energy up to $N = 45$.

To predict likely 'magic numbers' as a function of ρ_0 we have considered[42] the second difference of the energy, $\Delta_2 E = E(N+1) + E(N-1) - 2E(N)$. For $\rho_0 = 6$ the pattern is the same as for the LJ potential, with magic numbers at $N = 7$, 10, 13, 19 and 23. The last three values correspond to the single, double and triple icosahedron, respectively. For smaller ρ_0 the relative stability of M_7 and M_{10} disappears, and at still larger ρ_0 the magic number character of the icosahedron is also lost. For $\rho_0 = 14$ our results should be appropriate to C_{60} clusters and we predict a magic number at $n = 23$ corresponding to the complete decahedron.

We have also considered M_{38}, M_{46}, M_{55}, M_{70} and M_{75}, although for these sizes we cannot be confident that we have found the global minimum in each case.[42] For M_{38} at low ρ_0 our lowest minimum is distorted and highly strained. As ρ_0 increases structures based on icosahedra with anti-Mackay overlayers become most favourable; at shorter range, clusters with Mackay overlayers lie lower, but are never the lowest because the truncated octahedron shown in Fig. 10(*a*) is the global minimum over a wide range of ρ_0. It is noteworthy that the crossover from decahedral to f.c.c.-based global minima, based on extrapolation for magic number LJ clusters,[49] occurs at around $N \approx 10^5$. Our lowest minimum for M_{46} at long range is based on the 45-atom rhombic tricontahedron, but has an extra atom in the outer shell [Fig. 10(*b*)]. As ρ_0 increases our lowest minimum changed from an incomplete Mackay icosahedron to an incomplete decahedron and finally to a structure based on the 31-atom truncated tetrahedron.[42]

As discussed above, the 55-atom cluster is a magic number species for various atomic[9,50–53] and molecular systems.[51,54] The relative energies of Mackay icosahedra, Ino decahedra[26] and cuboctahedra have previously been compared for various potentials.[22,55,56] However, this may not provide the most useful comparison, because the Ino decahedron and the cuboctahedron are not necessarily the lowest-energy decahedral and f.c.c.-type structures. In both cases it is possible to construct less-symmetrical clusters of the same size with a smaller proportion of {100}-type facets. Marks' decahedra, with re-entrant {111} faces between the edges of the {100} faces,[57] and truncated octahedra or species with further facetting,[49] appear to be more favourable morphologies. For M_{55} the Ino decahedron and the cuboctahedron are never the lowest-energy decahedral or f.c.c. 55-atom clusters.[42] The most favourable f.c.c. clusters are instead based on the 31-atom truncated tetrahedron. As expected the lowest-energy minima

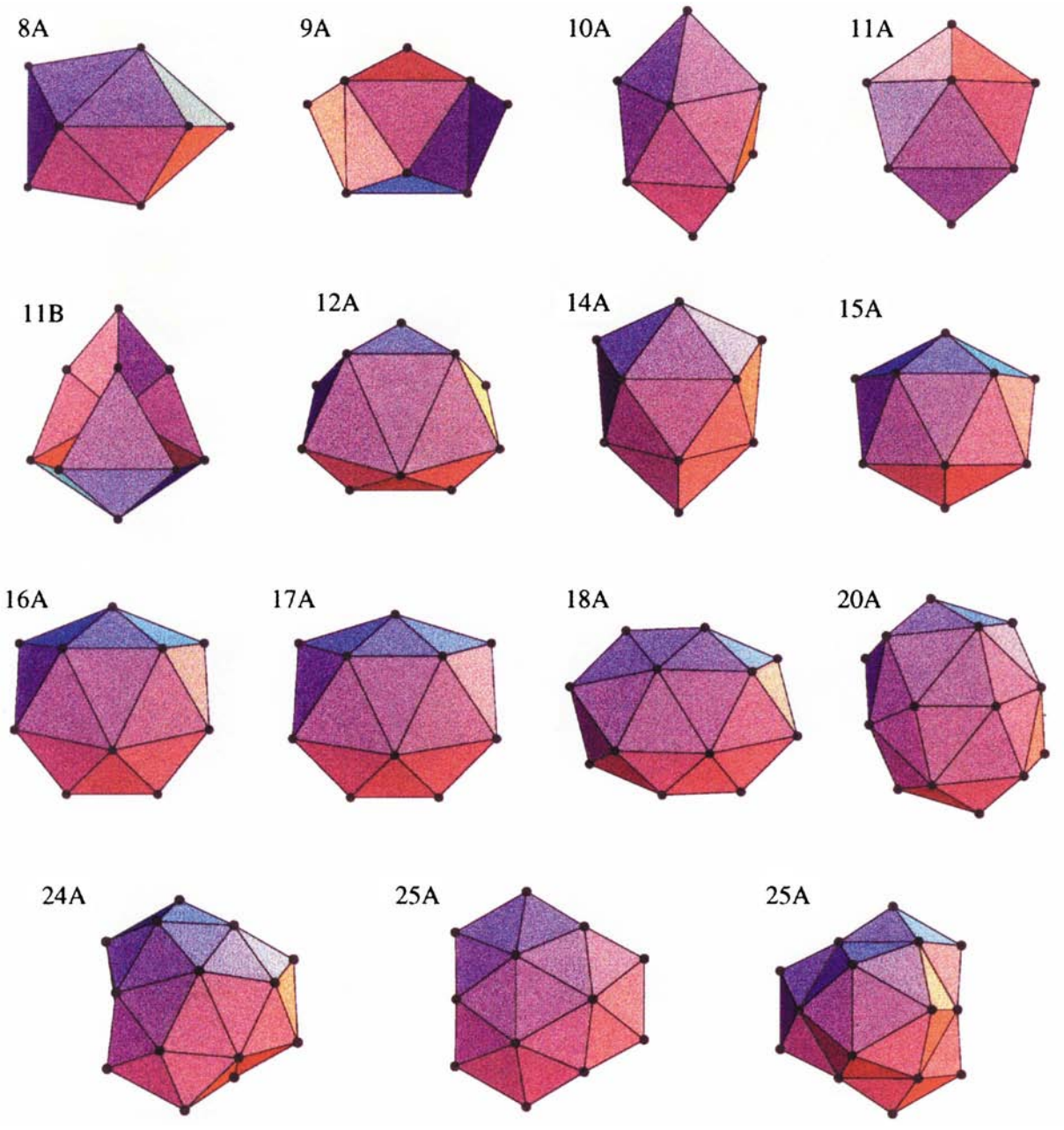

Fig. 5 Global minima associated with low values of ρ_0. Each structure is labelled by the symbol given in Table 1. The graphics were produced with MATHEMATICA[43] using a cut-off of 1.2 for triangulation

change from being based on icosahedra to decahedra and then to f.c.c.-type structures as the range decreases.

Similar patterns are seen for M_{70}, M_{75} and M_{79}. The most favourable structures based upon decahedra may be constructed from the 75-atom Marks' decahedron[57] shown in Fig. 10(*c*). The crossover from icosahedra to decahedra based on the magic number sequence for LJ clusters[49] is at $N \approx 1600$. Hence it is interesting that the 75-atom Marks' decahedron seems to be the global minimum for LJ_{75}. The f.c.c. clusters are based on the 79-atom truncated octahedron [Fig. 10(*d*)] which is close to the corresponding Wulff polyhedron.[58] We expect 'magic numbers' for potentials of appropriate range for the sequence of Marks' decahedra with $N = 75, 192, 389, \ldots$, the sequence of truncated octahedra with hexagonal faces and $N = 38, 201, 586, \ldots$, and perhaps for truncated octahedra with irregular hexagonal faces and $N = 79, 140, 314$.

Parks *et al.*[11-13] have made detailed studies of the structure of small nickel clusters using chemical probes. Nitrogen is a particularly useful probe, as it can be used to ascertain the number of surface atoms with a particular range of co-ordination number. From these data they have deduced the structure of bare nickel clusters with 3 to 28 and 49 to 71 atoms. Although the interpretation of the experimental results is not without ambiguity, they provide convincing evidence that the dominant morphology in these size ranges is icosahedral. However, there is some disparity between their results and the calculations of Stave and DePristo.[14] The experimental results are consistent with a shorter-ranged potential than that employed by the latter authors. Parks *et al.* find that growth on their 13- and 55-atom icosahedra starts in the anti-Mackay sites, but for Ni_{28} the surface has changed to a Mackay overlayer. This is a surprisingly small size for the Mackay overlayer to appear; for the LJ potential ($\rho_0 = 6$) the crossover in stability occurs at LJ_{31}.

Our results suggest alternative structures for Ni_{14} and Ni_{17} that were not considered by Parks *et al.* First, for Ni_{14} their proposal of a hollow, bicapped hexagonal antiprism[11] seems unlikely, as this structure is never a true minimum for the Morse potential at any range. A capped icosahedron with 12 surface sites that bind one N_2 molecule relatively strongly and one site (the cap) that binds two seems more likely to us. For Ni_{17}, Parks *et al.* dismiss one structure based upon icosahedral order (our

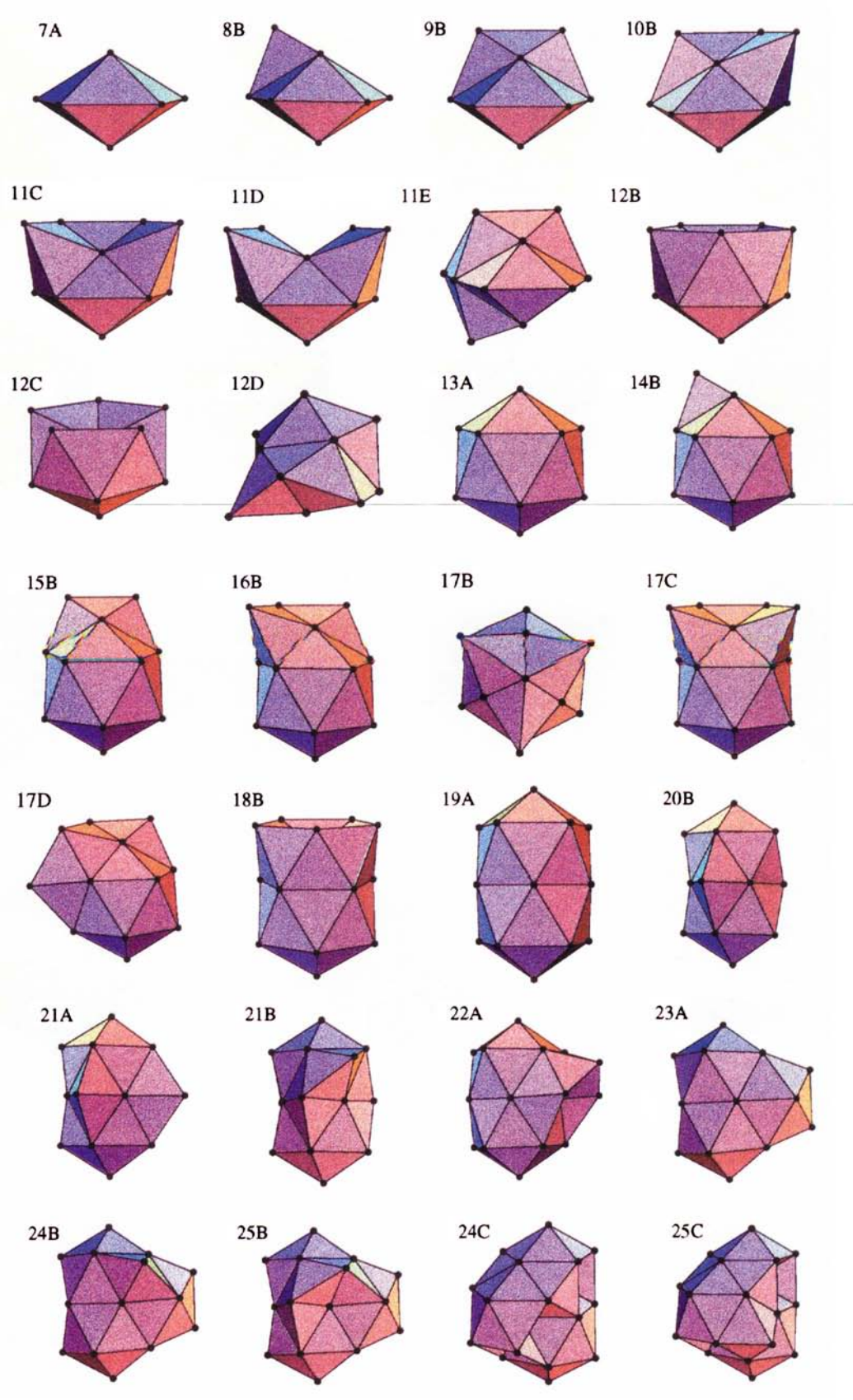

Fig. 6 Global minima based on icosahedral packing

17C) but did not consider isomers such as our 17B and 17D (Fig. 6) and instead proposed a non-icosahedral structure.[13]

Since our structural predictions here are based entirely on empirical potentials, with no explicit consideration of electronic structure or Jahn–Teller distortions, we must also ask when geometric rather than electronic effects may dominate. A crossover from electronic to geometric 'magic numbers' has apparently been seen in sodium clusters as the size increases.[59] Temperature-dependent spectra indicate that electronic magic numbers are seen for liquid-like clusters, and geometric magic numbers for solid-like clusters.[60] A similar temperature dependence has also been observed for aluminium clusters.[61] This behaviour matches that expected for clusters bound by a long-ranged Morse potential. For small clusters the lowest-

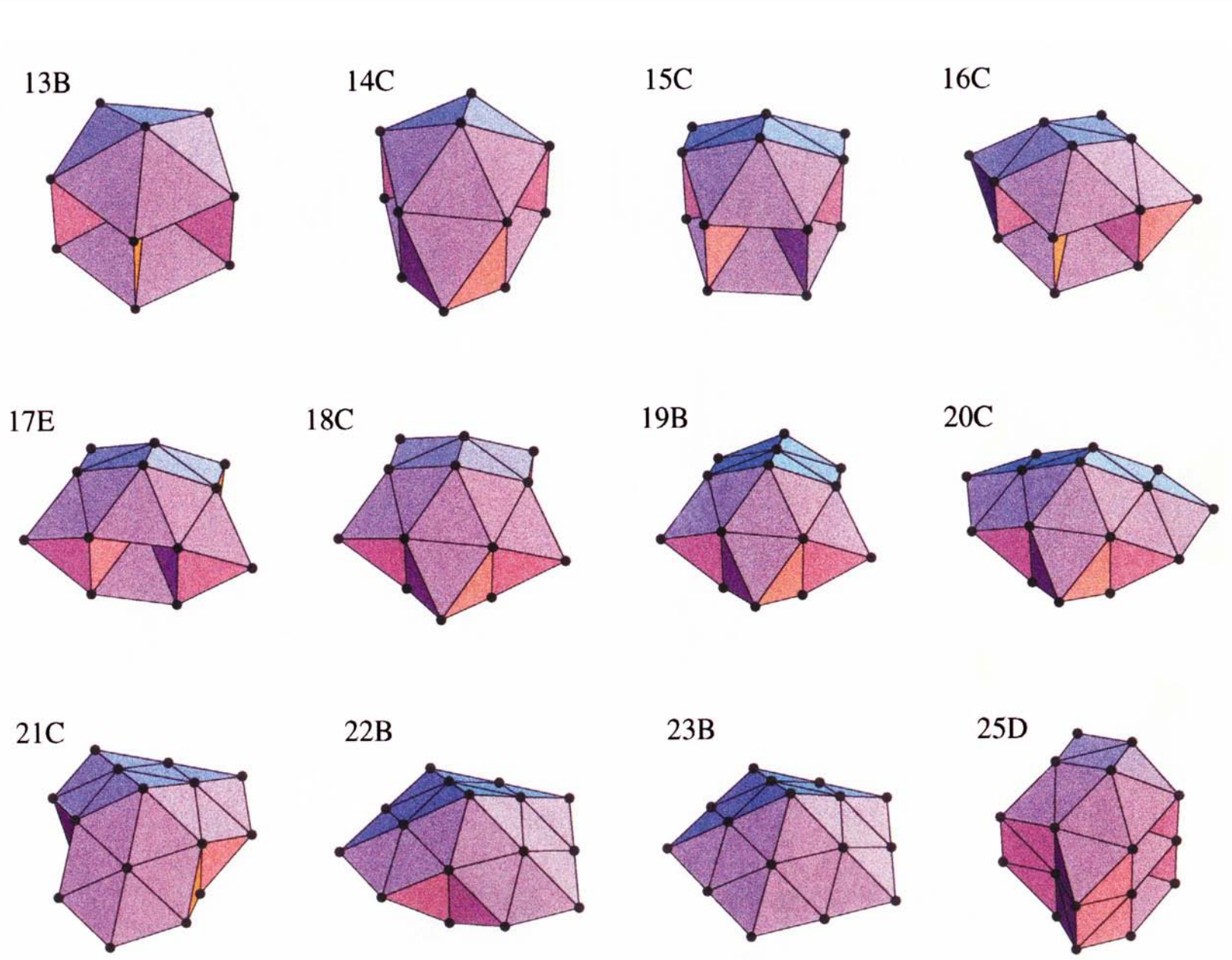

Fig. 7 Global minima based on decahedral packing

Fig. 8 Global minima based on close packing

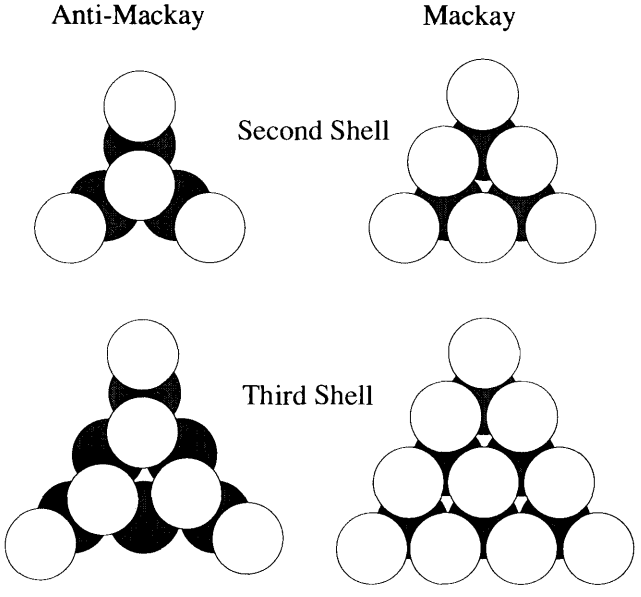

Fig. 9 Atomic positions for the two possible overlayers of the icosahedron, anti-Mackay (left) and Mackay (right). These are shown for a single face of the icosahedron

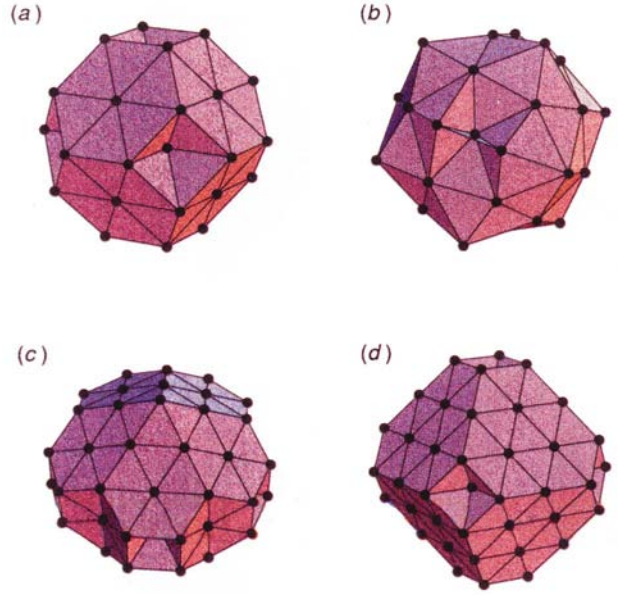

Fig. 10 (*a*) The M_{38} truncated octahedron. (*b*) The M_{46} minimum based on the 45-atom rhombic tricontahedron. (*c*) The M_{75} Marks' decahedron. (*d*) The M_{79} truncated octahedron

energy minima are amorphous and only a very low temperature is required for melting as the liquid-like band of minima is approximately continuous in energy. In this size range the clusters would exhibit electronic shell structure at all temperatures. However, as the size increases the liquid-like state should become less stable, until a critical size is reached at which the icosahedron becomes the ground state. Above this size the cluster would exhibit geometric shell structure as long as the temperature is below the melting point. For metals with shorter-ranged potentials, geometric rather than electronic magic numbers are likely to dominate at relatively small size. On the basis of Table 1 we tentatively suggest that this may be the case for nickel clusters.

Sutton–Chen and Murrell–Mottram Potentials

We now consider the rearrangement mechanisms of capped magic number clusters bound by the many-body Sutton–Chen[62] and the two- plus three-body Murrell–Mottram potentials,[63] parameterised for f.c.c. transition metals.[64] The results provide insight into the most favourable morphology of each cluster and also into the competition between dynamics and thermodynamics. In fact, fluctuations between cuboctahedral and icosahedral morphologies have been reported by electron microscopists.[65–67] Sawada and Sugano[68] investigated the corresponding energetics of Au_{55} and Au_{147} using a many-body Gupta potential.[69] They concluded that some additional effect is needed to explain the observation of cuboctahedra, and that this is most likely to be the interaction with the substrate. Although we have found that capping can have a similar effect we concur with this conclusion.

The Sutton–Chen (SC) potential has the form (8) where $\rho_i = \sum_{j \neq i}(a/r_{ij})^m$, c is a dimensionless parameter, ε a parameter with dimensions of energy, a the lattice constant and m and n are positive integers with $n > m$. We use the parameters given by Sutton and Chen[60] for the metals Ni, Ag and Au; Cu has the same scaled parameters as Ni, Rh the same as Ag and Pt the same as Au, so the corresponding results for these metals can simply be obtained from their partners by rescaling, as mentioned above. For Ni and Cu $n = 9$ and $m = 6$, for Ag and Rh $n = 12$ and $m = 6$ and for Au and Pt $n = 10$ and $m = 8$. The Sutton–Chen potential provides a reasonable description of various bulk properties,[62,70] with an approximate many-body representation of the delocalised metallic bonding. However, it does not include any directional terms, which are likely to be important for transition metals with partially occupied d shells.

$$E = \varepsilon \sum_i \left[\frac{1}{2} \sum_{j \neq i} \left(\frac{a}{r_{ij}} \right)^n - c\sqrt{\rho_i} \right] \quad (8)$$

The two- plus three-body Murrell–Mottram (MM) potential[63,71] may be written as in equation (9). In this case up to

$$V = \sum_i \sum_{j<i} V_{ij}^{(2)} + \sum_i \sum_{j<i} \sum_{k<j} V_{ijk}^{(3)} \quad (9)$$

around 15 parameters are fitted to bulk properties such as phonon frequencies, elastic constants, bulk cohesive energy, lattice constant and vacancy-formation energy.[63,71–73,*]

* The c_1 parameter for Cu in ref. 72 has the wrong sign.[74]

One obvious question which must be asked is how well potentials like these, which have been fitted to bulk properties, are likely to perform for clusters where most of the atoms find themselves in the surface.[75] Some clues are available from surface calculations. The SC potentials considerably underestimate surface energies, and give surface relaxations which are too large but of the right form.[76] The change in mechanism of the surface migration from bulk Pt (which occurs by surface exchange) to Rh (which occurs by simple migration) is correctly reproduced.[70] However, Hammonds[77] has concluded that the SC potentials do not support surface reconstructions of the top-layer contraction type, because the surfaces are too stable with respect to the bulk. On the other hand, SC potentials have been shown to reproduce step-roughening phenomena.[78] The inclusion of directional terms in the MM potentials improves results for the bulk over those for SC and gives better surface energies, but surface relaxations are underestimated.[72]

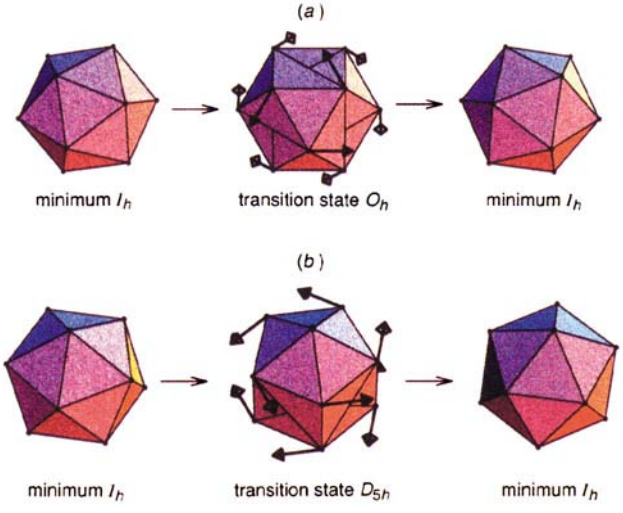

Fig. 11 (*a*) The 6DSD process for SC Ag_{13}. (*b*) The 5DSD process for SC Ag_{13}. The clusters were triangulated using a distance cut-off criterion and the transition vector (*i.e.* the displacements corresponding to the normal mode with the unique imaginary frequency) is superimposed on the transition state

For the present results direct comparison with experimental mechanisms is not usually possible. However, we can compare our calculated rate constants with the lifetimes observed for cuboctahedral and icosahedral gold clusters using electron microscopy. We can also test some of our results against calculations using the embedded-atom model[79] and effective medium theory.[80] Where we identify rearrangements which correspond to surface diffusion, it is often possible to make comparisons with experimental or theoretical results for analogous processes on bulk surfaces. We have found cluster analogues of terrace diffusion, exchange processes and diffusion over edges which are important in understanding homoepitaxial growth, island formation and diffusion-limited aggregation.[81–84]

For the 'magic number' 13-, 55- and 147-atom clusters we have identified a number of highly co-operative processes.[64] For 13 atoms the cuboctahedron and decahedron are both true transition states for degenerate rearrangements of the icosahedron for all potentials, with the decahedron lower in energy. (A degenerate rearrangement is one in which the two minima differ only by permutations of atoms of the same element.[85])

The MM decahedra are higher index saddles for the larger sizes, whilst the corresponding SC decahedra are minima. For SC Ag_{13} and Au_{13} the icosahedron is the global minimum of energy according to previous geometry optimisations[22] and systematic quenching from molecular dynamics trajectories.[86]

Mackay probably first described the direct geometrical transformation of a cuboctahedron into an icosahedron.[25] In this process one of the diagonals of each square face is contracted and the faces are folded along the same diagonal to give two equilateral triangles. The rearrangement of each square face is related to Lipscomb's diamond–square-diamond (DSD) mechanism[23] [Fig. 2(*a*)], which was first proposed in the context of borohydride chemistry. Mackay's transformation

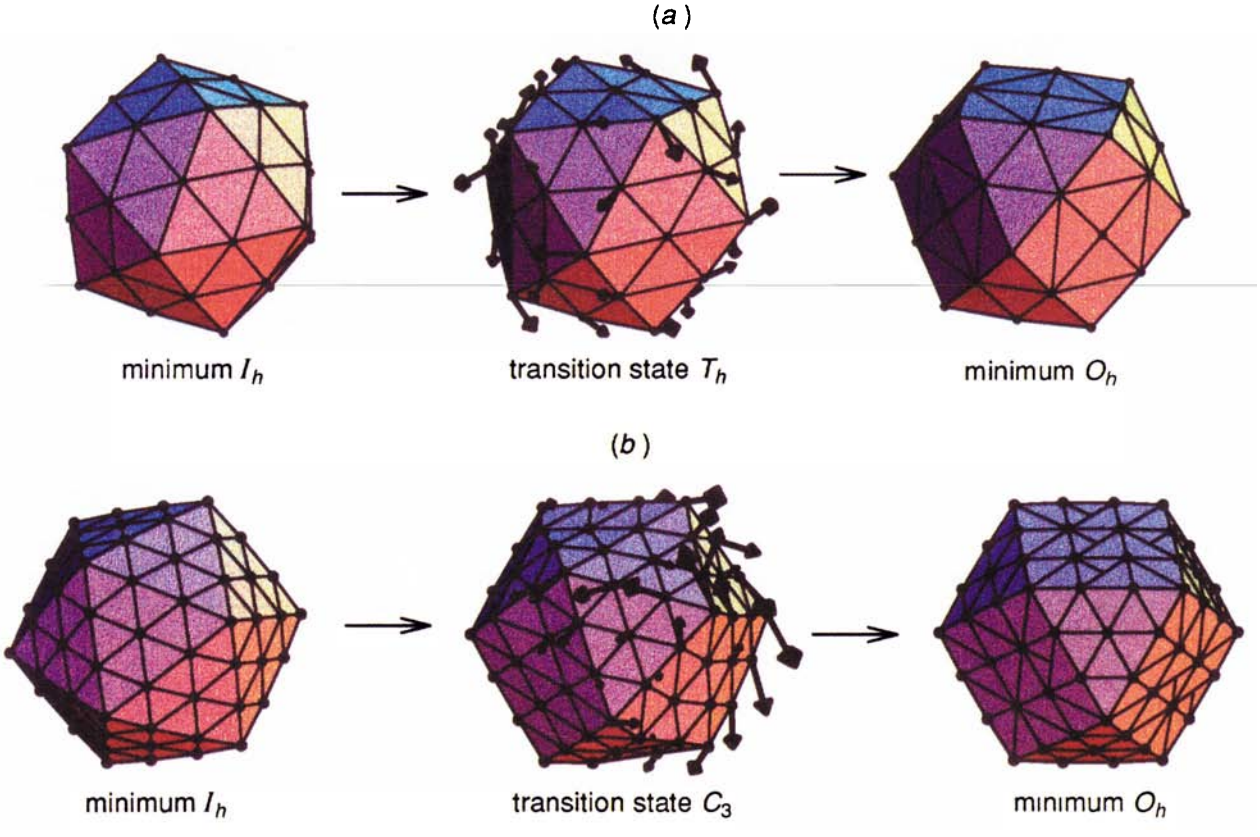

Fig. 12 The 6DSD process (*a*) in SC Au_{55} *via* a T_h transition state and (*b*) in SC Au_{147} *via* a C_3 transition state

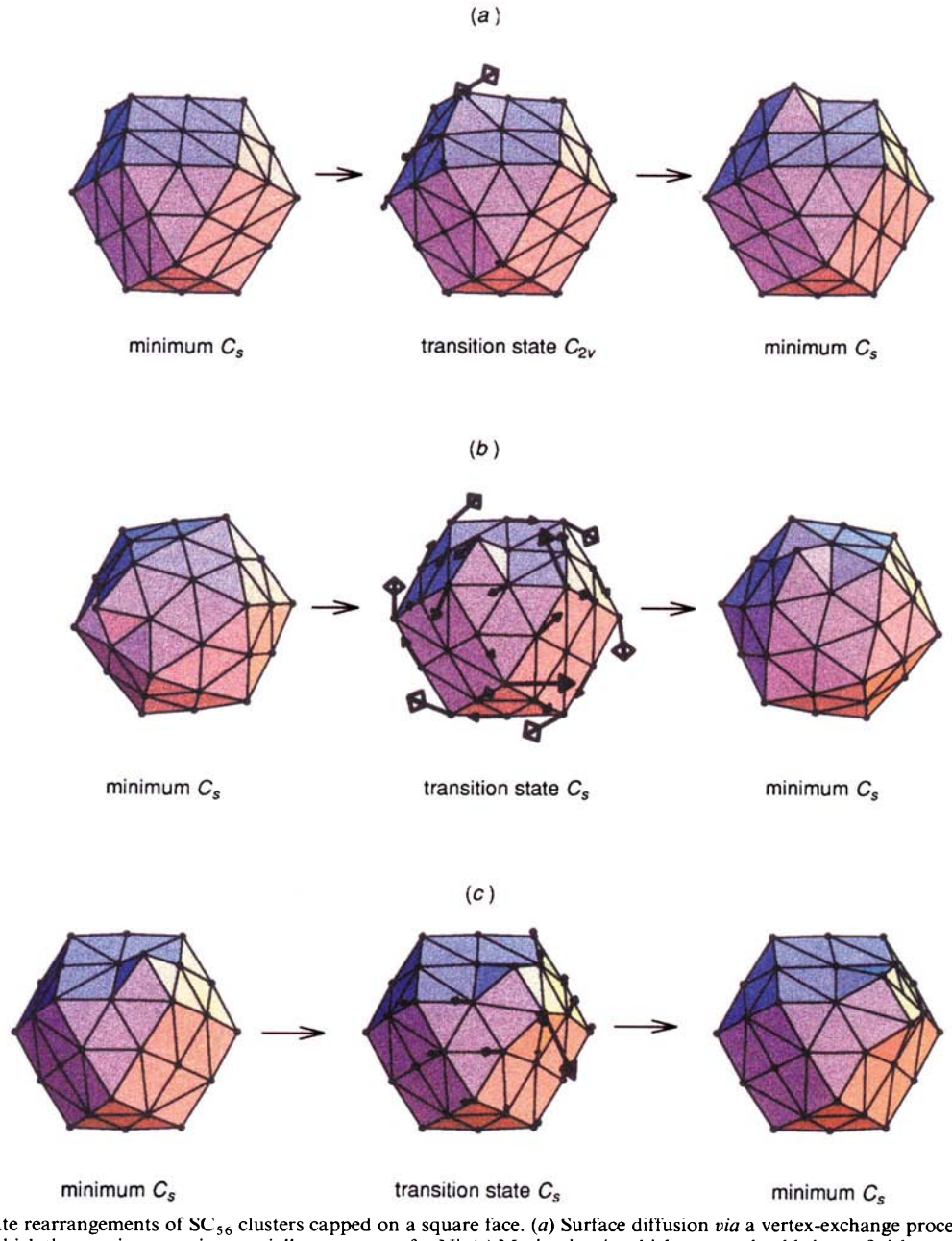

Fig. 13 Degenerate rearrangements of SC_{56} clusters capped on a square face. (*a*) Surface diffusion *via* a vertex-exchange process for Ag. (*b*) The 6DSD process in which the capping atom is essentially a spectator for Ni. (*c*) Mechanism in which a capped gold cluster finishes at a minimum where two atoms essentially share a vertex site

from one icosahedron to another *via* a cuboctahedron can therefore be described in terms of a concerted sextuple diamond–square–diamond (6DSD) mechanism [Fig. 11(*a*)]. There is another highly co-operative mechanism which can permute icosahedra in a different way. In this case the transition state is a decahedron (D_{5h} symmetry) and the concerted process corresponds to a quintuple DSD process (5DSD) [Fig. 11(*b*)].

For the potentials and the sizes considered here the icosahedron is always lower in energy than the cuboctahedron. This is consistent with the calculations for Ni by Cleveland and Landman[87] using an embedded-atom potential and with the electron microscopy results of Doraiswamy and Marks[88] who studied small gold particles on an SiO support. Our results are also consistent with those of Vlachos *et al.*[89] who also considered the relative energetics of cuboctahedra and icosahedra. We find that MM_{55} and SC Ni_{55} cuboctahedra are transition states, whilst SC Ag_{55} and Au_{55} cuboctahedra are true minima which can rapidly transform to icosahedra *via* T_h symmetry transition states.[64] The stability of the icosahedral morphology in this size range is also in general agreement with the chemical probe results of Parks and co-workers mentioned above.[8–13,90] However, for SC Au_{55} quenching has previously shown that the lowest-energy minima generally have little symmetry and lie below both the icosahedron and the cuboctahedron.[86] This is due to the short range of this potential.[42]

For the larger SC clusters, the single-step co-operative mechanisms are replaced by two-step processes except for Ni_{55}. In such cases the decahedron or cuboctahedron becomes a minimum, and there must be at least one transition state of lower symmetry in between. For the cuboctahedron this change in morphology can occur *via* a single T_h transition state [Fig. 12(*a*)], as found previously[38] for $(C_{60})_{55}$, or *via* a C_3 transition state [Fig. 12(*b*)].

The barrier to the 6DSD process scales roughly as the number of atoms for each MM potential. However, with increasing size we expect the cuboctahedron to become a minimum and the overall O_h to I_h transformation to occur *via* a sequence of transition states, as for the larger SC clusters. For both classes of potential, our calculated rate constants indicate that cuboctahedra should not be observable at experimentally

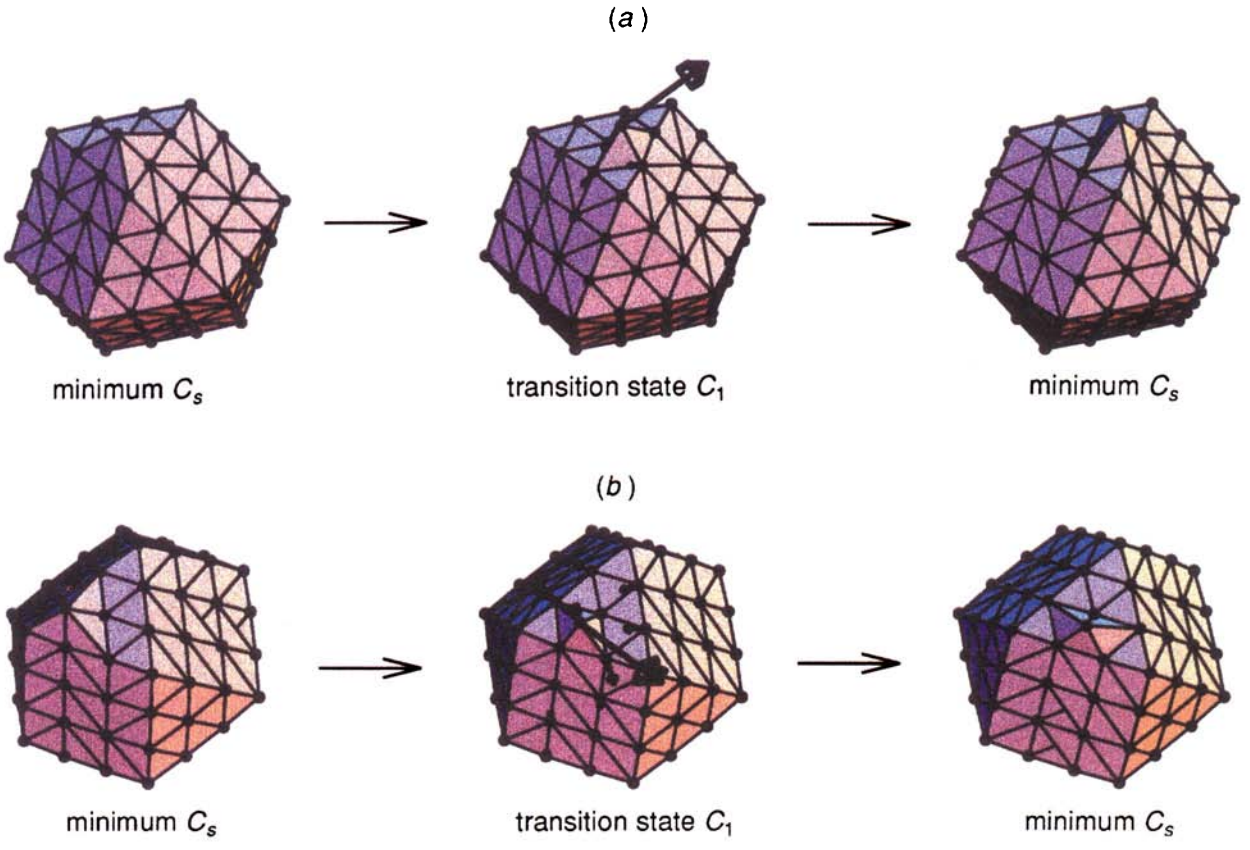

Fig. 14 Rearrangements of SC_{148} clusters showing surface migration of the cap *via* an edge-bridging transition state in (*a*) Ag_{148} and (*b*) Ni_{148}. In fact these are really different views of the same mechanism

relevant temperatures for Au_{55} and Au_{147}. These results do not agree with the experimental observations; Sawada and Sugano reached the same conclusion and were therefore led to suggest that interaction with the substrate might preferentially stabilise these cuboctahedra.

For capped magic number clusters the mechanisms are not always clear-cut, but may broadly be divided into rearrangements that are surface migrations of capping atoms and co-operative rearrangements of the underlying cluster where the capping atom is essentially a spectator. For MM clusters in particular, the latter processes dominate,[64] except for Cu. For the large SC clusters, on the other hand, we mostly found surface migrations after capping. Some examples are shown in Fig. 13. In some cases capping turns a structure which was a transition state into a minimum, and the reaction path must split into two, each part mediated by a new transition state. Capping always reduces the barrier to the 6DSD process in MM_{56} clusters and in SC Ni_{56}; the associated frequency factors do not change much from the magic number rearrangements.

For the 148-atom clusters we found only surface migrations for SC Au_{148}, only 6DSD processes for MM Ag_{148} and Au_{148} and both surface and co-operative processes for the others. Two examples are shown in Fig. 14; in each case an edge-bridging process [24] results in migration over the same {100}-type face of a cuboctahedron. We have also found mechanisms where atoms migrate between faces of the cluster, either by edge-bridging (Fig. 15) or exchange-type processes.

We have compared our results with experiment and previous theoretical calculations as far as possible, exploiting the analogous migration processes for bulk surfaces where possible.[64] It seems unlikely that a single capping atom could stabilise the Au_{55} and Au_{147} cuboctahedra sufficiently to account for the experimental observations discussed above. Sawada and Sugano's suggestion that the substrate interaction is responsible still seems the most plausible.

We note that surface-diffusion processes generally have lower barriers and frequency factors than do the co-operative rearrangements. Hence we expect most of the surface migrations to have significant rate constants at room temperature. In contrast, changes in morphology from the icosahedron *via* concerted rearrangements are very unlikely to be seen at room temperature. This suggests that icosahedral order will be 'frozen in', and hence kinetic rather than thermodynamic products may be observed in molecular beam experiments for clusters of more than around 10^3 atoms. In general our results agree quite well with those for similar processes in bulk systems as detailed elsewhere.[64]

Conclusion

In this contribution we have considered the structure and rearrangement mechanisms predicted for clusters bound by four classes of empirical interatomic potential. The model anisotropic LJAT potential can support structures ranging from close packed to rings and chains as a function of a single parameter. Matching an experimental structure to a given minimum for this potential can then provide a first guess of the sorts of rearrangements the cluster may undergo. We also predict that cuboctahedra will become more energetically favourable as the magnitude of the anisotropy increases.

The Morse potential has a single adjustable parameter which governs the range of the atomic interaction. Very long-range potentials, which appear to be appropriate for alkali metals, result in amorphous global minima. As the range decreases first icosahedral, then decahedral and finally f.c.c. morphologies are the most favourable. These crossovers, as well as the relative importance of geometric *versus* electronic effects in determining structure, can all be understood in terms of the strain energy. A short-ranged potential destabilises strained geometries such as the icosahedron. Comparison with experiment suggests that a relatively short-ranged potential is appropriate for Ni.

Two classes of potential specifically parameterised for f.c.c.

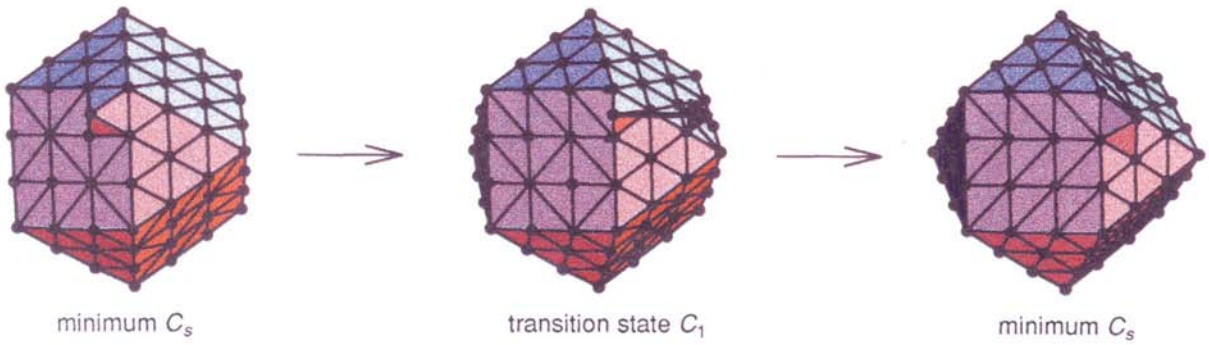

Fig. 15 Surface rearrangement of an SC Ag_{148} cluster in which the cap moves between facets *via* an edge-bridging transition state

transition metals have also been considered. In both cases icosahedra generally have lower energy than cuboctahedra and highly co-operative rearrangements exist, especially for smaller clusters. As the nuclearity increases the single-step co-operative pathways break down into multiple steps, each one mediated by a new transition state. Both potentials predict that Au_{55} and Au_{147} cuboctahedra should not be observable experimentally, in contradiction to results from electron microscopy.[65,67] The discrepancy is probably due to a substrate interaction, as suggested by Sawada and Sugano.[68]

Both classes of potential suggest that co-operative changes in morphology will not occur at an appreciable rate for the larger sizes considered here under a wide range of experimental conditions. Hence we predict that icosahedral order is likely to be frozen in to bigger clusters which grow from such nuclei. Surface migrations, on the other hand, are likely to have appreciable rates at reasonable temperatures. Therefore we expect anti-Mackay overlayers to be formed initially, which convert through surface migrations into Mackay overlayers when the number of atoms increases. This means that the continued growth of Mackay icosahedra on an underlying template should be possible, until the strain becomes intolerable.

Acknowledgements

We gratefully acknowledge financial support from the Royal Society (to D. J. W.) and the EPSRC (to J. P. K. D. and L. J. M.).

References

1 O. D. Haberlen, S. C. Chung and N. Rösch, *Int. J. Quant. Chem.*, 1994, **S28**, 595.
2 J. P. Lu and W. T. Yang, *Phys. Rev. B*, 1994, **49**, 11 421.
3 D. York, J. P. Lu and W. T. Yang, *Phys. Rev. B*, 1994, **49**, 8526.
4 W. T. Yang, *Theochem.*, 1992, **87**, 461.
5 M. R. Hoare and J. McInnes, *Faraday Discuss. Chem. Soc.*, 1976, **61**, 12.
6 F. H. Stillinger and T. A. Weber, *Phys. Rev. A*, 1982, **25**, 978.
7 F. H. Stillinger and T. A. Weber, *Science*, 1984, **225**, 983.
8 E. K. Parks, B. J. Winter, T. D. Klots and S. J. Riley, *J. Chem. Phys.*, 1991, **94**, 1882.
9 T. D. Klots, B. J. Winter, E. K. Parks and S. J. Riley, *J. Chem. Phys.*, 1991, **95**, 8919.
10 E. K. Parks, B. J. Winter, T. D. Klots and S. J. Riley, *J. Chem. Phys.*, 1992, **96**, 8267.
11 E. K. Parks, L. Zhu, J. Ho and S. J. Riley, *J. Chem. Phys.*, 1994, **100**, 7206.
12 E. K. Parks and S. J. Riley, *Z. Phys. D*, 1995, **33**, 59.
13 E. K. Parks, L. Zhu, J. Ho and S. J. Riley, *J. Chem. Phys.*, 1995, **102**, 7377.
14 M. S. Stave and A. E. DePristo, *J. Chem. Phys.*, 1992, **97**, 3386.
15 J. Jellinek and Z. B. Güvenç, in *The Synergy between Dynamics and Reactivity at Clusters and Surfaces*, ed. L. J. Farrugia, Kluwer, Dordrecht, 1995, p. 217.
16 D. J. Wales, *J. Chem. Phys.*, 1994, **101**, 3750.
17 J. E. Jones and A. E. Ingham, *Proc. R. Soc. London, Ser. A*, 1925, **107**, 636.
18 F. Ercolessi, M. Parrinello and E. Tosatti, *Philos. Mag. A*, 1988, **58**, 213; V. Vitek and D. J. Srolovitz (Editors), *Atomistic Simulation of Materials: Beyond Pair Potential*, Plenum, New York, 1989.
19 L. G. M. Petersson, C. W. Bauschlicher and T. Halicioglu, *J. Chem. Phys.*, 1987, **87**, 2205; S. Erkoc and S. Katircioglu, *Chem. Phys. Lett.*, 1988, **147**, 476; D. K. Choi, S. M. Koch, T. Takai, T. Halicioglu and W. A. Tiller, *J. Vac. Sci. Technol. B*, 1988, **6**, 1140; T. Halicioglu, H. O. Pamuk and S. Erkoc, *Phys. Status Solidi B*, 1988, **149**, 81; H. Balamore, T. Halicioglu and W. A. Tiller, *Phys. Rev. B*, 1989, **40**, 9999; T. Halicioglu and H. O. Pamuk, *Surf. Sci.*, 1989, **215**, 272; T. Halicioglu and P. J. White, *Surf. Sci.*, 1981, **106**, 45.
20 B. M. Axilrod and E. Teller, *J. Chem. Phys.*, 1943, **11**, 299; B. M. Axilrod, *J. Chem. Phys.*, 1949, **17**, 1349; 1951, **19**, 719.
21 D. J. Wales, *J. Chem. Soc., Faraday Trans.*, 1990, **86**, 3505; J. P. K. Doye and D. J. Wales, *J. Chem. Soc., Faraday Trans.*, 1992, **88**, 3295.
22 J. Uppenbrink and D. J. Wales, *J. Chem. Phys.*, 1992, **96**, 8520.
23 W. N. Lipscomb, *Science*, 1966, **153**, 373.
24 B. F. G. Johnson, *J. Chem. Soc., Chem. Commun.*, 1986, **27**.
25 A. L. Mackay, *Acta Crystallogr*, 1962, **15**, 916.
26 S. Ino, *J. Phys. Soc. Jpn.*, 1969, **27**, 941.
27 P. M. Morse, *Phys. Rev.*, 1929, **34**, 57.
28 L. A. Girifalco and V. G. Weizer, *Phys. Rev.*, 1959, **114**, 687.
29 K. P. Huber and G. Herzberg, *Constants of Diatomic Molecules*, Van Nostrand Reinhold, New York, 1979.
30 P. A. Braier, R. S. Berry and D. J. Wales, *J. Chem. Phys.*, 1990, **93**, 8745.
31 M. R. Hoare and J. McInnes, *Adv. Phys.*, 1983, **32**, 791.
32 J. Rose and R. S. Berry, *J. Chem. Phys.*, 1993, **98**, 3262.
33 F. H. Stillinger and D. K. Stillinger, *J. Chem. Phys.*, 1990, **93**, 6106.
34 F. H. Stillinger and T. A. Weber, *J. Stat. Phys.*, 1988, **52**, 1429.
35 I. Bytheway and D. L. Kepert, *J. Math. Chem.*, 1992, **9**, 161.
36 L. A. Girifalco, *J. Phys. Chem.*, 1992, **96**, 858.
37 D. J. Wales and J. Uppenbrink, *Phys. Rev. B*, 1994, **50**, 12 342.
38 D. J. Wales, *J. Chem. Soc., Faraday Trans.*, 1994, **90**, 1061; *J. Chem. Phys.*, 1994, **101**, 3750.
39 C. Rey, L. J. Gallego and J. A. Alonso, *Phys. Rev. B*, 1994, **49**, 8491.
40 A. Cheng, M. L. Klein and C. Caccamo, *Phys. Rev. Lett.*, 1993, **71**, 1200.
41 M. H. J. Hagen, E. J. Meijer, G. C. A. Mooij, D. Frenkel and H. N. W. Lekkerkerker, *Nature (London)*, 1993, **365**, 425; C. Caccamo, *Phys. Rev. B*, 1995, **51**, 3387.
42 J. P. K. Doye, D. J. Wales and R. S. Berry, *J. Chem. Phys.*, 1995, **103**, 4234.
43 S. Wolfram, MATHEMATICA, Addison-Wesley, Redwood City, 2nd edn. 1991.
44 J. A. Northby, *J. Chem. Phys.*, 1987, **87**, 6166.
45 See, for example, R. Williams, *The Geometrical Foundation of Natural Structure*, Dover, New York, 1972.
46 M. R. Hoare, *Adv. Chem. Phys.*, 1979, **40**, 49.
47 J. Farges, M. F. de Feraudy, B. Raoult and G. Torchet, *J. Chem. Phys.*, 1983, **78**, 5067; 1986, **84**, 3491; *Adv. Chem. Phys.*, 1988, **70**, 45.
48 M. Sung, R. Kawai and J. H. Weare, *Phys. Rev. Lett.*, 1994, **73**, 3552.
49 B. Raoult, J. Farges, M. F. de Feraudy and G. Torchet, *Z. Phys. D*, 1989, **12**, 85; *Philos. Mag. B*, 1989, **60**, 881.
50 O. Echt, K. Sattler and E. Recknagel, *Phys. Rev. Lett.*, 1981, **47**, 1121.
51 K. E. Schriver, M. Y. Hahn, J. L. Persson, M. E. LaVila and R. L. Whetten, *J. Phys. Chem.*, 1989, **93**, 2869.
52 T. D. Klots, B. J. Winter, E. K. Parks and S. J. Riley, *J. Chem. Phys.*, 1990, **92**, 2110.
53 M. Pellarin, B. Baguenard, J. L. Vialle, J. Lermé, M. Broyer, J. Miller and A. Perez, *Chem. Phys. Lett.*, 1994, **217**, 349.

54 O. Echt, O. Kandler, T. Leisner, W. Miehle and E. Recknagel, *J. Chem. Soc., Faraday Trans.*, 1990, **86**, 2411.
55 Q. Wang, M. D. Glossman, M. P. Iniguez and J. A. Alonso, *Philos. Mag. B*, 1994, **69**, 1045.
56 H. S. Lim, C. K. Ong and F. Ercolessi, *Surf. Sci.*, 1992, **269/270**, 1109.
57 L. D. Marks, *Philos. Mag. A*, 1984, **49**, 81.
58 G. Wulff, *Z. Kristallogr.*, 1901, **34**, 449.
59 T. P. Martin, T. Bergmann, H. Göhlich and T. Lange, *Chem. Phys. Lett.*, 1990, **172**, 209.
60 T. P. Martin, U. Näher, H. Schaber and U. Zimmerman, *J. Chem. Phys.*, 1994, **100**, 2322.
61 B. Baguenard, M. Pellarin, J. Lermé, J. L. Vialle and M. Broyer, *J. Chem. Phys.*, 1994, **100**, 754.
62 A. P. Sutton and J. Chen, *Philos. Mag. Lett.*, 1990, **61**, 139.
63 J. N. Murrell and R. E. Mottram, *Mol. Phys.*, 1990, **69**, 571.
64 D. J. Wales and L. J. Munro, *J. Phys. Chem.*, in the press.
65 P. M. Ajayan and L. D. Marks, *Phys. Rev. Lett.*, 1989, **63**, 279.
66 S. Iijima and T. Ichihashi, *Phys. Rev. Lett.*, 1986, **56**, 616.
67 D. J. Smith, A. K. Petford-Long, L. R. Wallenberg and J. O. Bovin, *Science*, 1986, **233**, 872.
68 S. Sawada and S. Sugano, *Z. Phys. D*, 1992, **24**, 37; 1991, **20**, 259.
69 R. P. Gupta, *Phys. Rev. B*, 1981, **23**, 6265.
70 R. M. Lynden-Bell, *Surf. Sci.*, 1991, **259**, 129.
71 S. D. Li, R. L. Johnston and J. N. Murrell, *J. Chem. Soc., Faraday Trans.*, 1992, **88**, 1229.
72 J. Uppenbrink, R. L. Johnston and J. N. Murrell, *Surf. Sci.*, 1994, **304**, 223.
73 J.-Y. Fang, R. L. Johnston and J. N. Murrell, *J. Chem. Soc., Faraday Trans.*, 1993, **89**, 1659.
74 J. Uppenbrink, personal communication.
75 W. Andreoni and G. Pastore, *Phys. Rev. B*, 1990, **41**, 10243.
76 B. D. Todd and R. M. Lynden-Bell, *Surf. Sci.*, 1993, **281**, 191.
77 K. D. Hammonds, *Mol. Phys.*, 1994, **81**, 227.
78 K. D. Hammonds and R. M. Lynden-Bell, *Surf. Sci.*, 1992, **278**, 437.
79 M. S. Daw, S. M. Foiles and M. I. Baskes, *Mater. Sci. Rep.*, 1993, **9**, 251.
80 K. W. Jacobsen, J. K. Nørskov and M. J. Puska, *Phys. Rev. B*, 1987, **35**, 7423.
81 Y. Li and A. E. DePristo, *Surf. Sci.*, 1994, **319**, 141.
82 J. Jacobsen, K. W. Jacobsen, P. Stoltze and J. K. Nørskov, *Phys. Rev. Lett.*, 1995, **74**, 2295.
83 H. X. Shao, S. D. Liu and H. Metiu, *Phys. Rev. B*, 1995, **51**, 7827.
84 H. Röder, K. Bromann, H. Brune and K. Kern, *Phys. Rev. Lett.*, 1995, **74**, 3217.
85 R. E. Leone and P. V. R. Schleyer, *Angew. Chem., Int. Ed. Engl.*, 1970, **9**, 860.
86 J. Uppenbrink and D. J. Wales, *J. Chem. Phys.*, 1993, **98**, 5720.
87 C. L. Cleveland and U. Landman, *J. Chem. Phys.*, 1991, **94**, 7376.
88 N. Doraiswamy and L. D. Marks, *Philos. Mag. B*, 1995, **71**, 291.
89 D. G. Vlachos, L. D. Schmidt and R. Aris, *J. Chem. Phys.*, 1992, **96**, 6880, 6891.
90 B. J. Winter, E. K. Parks and S. J. Riley, *J. Chem. Phys.*, 1991, **94**, 8618.

Received 8*th August* 1995; *Paper* 5/06359K